Acta Oceanol. Sin., 2010, Vol. 29, No. 4, P. 21-27
DOI: 10.1007/s13131-010-0047-6
http://www.hyxb.org.cn
E-mail: hyxbe@263.net

Ocean color products retrieval and validation around China coast with MODIS

SUN Ling[1]*, GUO Maohua[2], WANG Xiaomei[2]

[1] Key Laboratory of Radiometric Calibration and Validation for Environmental Satellites, China Meteorological Administration (LRCVES/CMA), National Satellite Meteorological Center, China Meteorological Administration, Beijing 100081, China

[2] National Satellite Ocean Application Service, State Oceanic Administration, Beijing 100081, China

Received 22 May 2009; accepted 14 December 2009

Abstract
Waters along China coast are very turbid with high concentrations of suspended sediment nearly all the time, especially at the Hangzhou Bay, the Changjiang (Yangtze) River Estuary and the shoal along Jiangsu Province. In these turbid and optically complex waters, the standard MODIS ocean color products tend to have invalid values. Because the water-leaving radiances in the near-infrared (NIR) are significant resulting from the strong scattering of suspended particles, the standard MODIS atmospheric correction algorithm often gets no results or produces significant errors. And because of the complex water optical properties, the OC3 model used in the standard MODIS data processing tends to get extremely high chlorophyll-a (Chl-a) concentrations. In this paper, we present an atmospheric correction approach using MODIS short wave infrared (SWIR) bands based on the fact that water-leaving radiances are negligible in the SWIR region because of the extreme strong absorption of water even in turbid waters. A regional Chl-a concentration estimation model is also constructed for MODIS from in situ data. These algorithms are applied to MODIS Aqua data processing in the China coastal regions. In situ data collected in the Yellow Sea and the East China Sea in spring and autumn, 2003 are used to validate the performance. Reasonably good results have been obtained. It is noted that water-leaving reflectance in the NIR bands are significant in waters along the China coast with high sediment loadings. The satellite derived and in-situ reflectance spectra can match in the turbid waters along China coast, and there is relatively good linear relationship between satellite derived and in-situ reflectance. The RMSE value of Rrs(λ) is 0.0031 sr^{-1} for all the nine ocean color bands (412 to 869 nm). The satellite-derived Chl-a value is in the reasonable range and the root mean square percentage difference is 46.1%.

Key words: ocean color, atmospheric correction, chlorophyll-a, MODIS, China coastal region, validation

1 Introduction

There are some of the most highly turbid coastal waters in the world along the China coastal region, especially in Hangzhou Bay, the Yangtze River Estuary and the shoal along Jiangsu province, with consistently high concentrations of suspended sediment and complex optical properties. The performance of standard MODIS ocean color processing is poor in this region. There remain some issues related to the atmospheric correction and water constituent concentration estimation, e.g., chlorophyll a (Chl-a). The sensor-derived water-leaving radiances at the blue bands (e.g., 412 and 443 nm) are often biased low and sometimes even go negative, which often results from turbid waters with significant ocean radiance contributions at the near-infrared (NIR) bands (Siegel et al., 2000). The sensor-derived Chl-a concentration is often highly overestimated as the result of both biased water-leaving reflectance spectrum and estimation model not suitable for these complex waters.

In the standard MODIS atmospheric correction, black ocean assumption at the two NIR bands (748 and 869 nm) is adopted for the open ocean (Gordon and Wang, 1994; Gordon, 1997). However, due to the strong scattering of suspended particles, the water-leaving radiances in the NIR bands are significant for turbid waters. Algorithm modifications to account for

Foundation item: The National Natural Science Foundation project of China under contract No. 40606043; the National Basic Research Program of China under contract No. 2006CB403702.
*Corresponding author, E-mail: sunling@cma.gov.cn

the NIR ocean contributions for productive waters have been implemented (Ruddick et al., 2000; Siegel et al, 2000; Stumpf et al., 2003; Lavender et al., 2005), but their performances in turbid coastal regions are still not good. Based on the fact that water has much stronger absorption at the short wave infrared (SWIR) wavelengths than the NIR wavelengths, the water-leaving radiances are generally negligible at the SWIR bands even for very turbid ocean waters. The SWIR atmospheric correction approach has been developed based on the standard MODIS algorithm (Wang, 2007) and applied to the turbid China east coastal region obtaining reasonably good results (Wang et al., 2007).

In the standard MODIS ocean color processing, the OC3 model is used for Chl-a concentration estimation (O'Reilly et al., 1998). However, due to the local features of ocean optical properties, this model is not proper for the turbid China coastal waters (Sun et al., 2009). Regional model should be constructed.

In this paper, an atmospheric correction algorithm using SWIR bands and a regional Chl-a estimation model are presented for MODIS. The ocean color products derived from MODIS Aqua data using these algorithms are reported and validated with in situ data collected in the Yellow Sea and the East China Sea.

2 Retrieval algorithms

2.1 *Atmospheric correction algorithm*

For the ocean-atmosphere system, the top-of-atmosphere (TOA) reflectance measured by the satellite sensor in a spectral band centred at a wavelength λ, $\rho_{\rm t}(\lambda)$, can be written as a linear sum of various contributions (angular dependencies are omitted):

$$\rho_{\rm t}(\lambda) = [\rho_{\rm w}(\lambda) + \rho_{\rm wc}(\lambda) + \rho_{\rm g}(\lambda)] T_{\rm g}(\lambda)T_{\rm r+a}(\lambda) + \rho_{\rm atm}(\lambda), \quad (1)$$

$$\rho_{\rm atm}(\lambda) = [\rho_{\rm mix}(\lambda) - \rho_{\rm r}(\lambda)] T_{\rm g}(\lambda) + \rho_{\rm r}(\lambda)T'_{\rm g}(\lambda), \quad (2)$$

where $\rho_{\rm w}$ is water-leaving reflectance, $\rho_{\rm wc}$ is whitecap reflectance, $\rho_{\rm g}$ is sun glint reflectance, $T_{\rm g}$ is gaseous absorption transmittance, $T'_{\rm g}$ is gaseous absorption transmittance excluding water vapour, $T_{\rm r+a}$ is scattering transmittance of the Rayleigh and aerosol mixing atmosphere, $\rho_{\rm atm}$ is intrinsic atmospheric reflectance reaching the sensor, $\rho_{\rm mix}$ is reflectance for the Rayleigh and aerosol mixing atmosphere not accounting for absorptive gases, and $\rho_{\rm r}$ is reflectance for a pure Rayleigh atmosphere not accounting for absorptive gases.

None water-leaving effects are calculated and removed from ρ_t to extract $\rho_{\rm w}$. $\rho_{\rm r}$ is calculated using look-up tables with angles and surface pressure (Sun et al., 2006). $T_{\rm g}$ together with $T'_{\rm g}$ is calculated using formulas based on simulations with angles and gases amounts (Sun and Zhang, 2007). $\rho_{\rm wc}$ is estimated using an empirical model with wind speed (Koepke, 1984; Gordon, 1997). $\rho_{\rm g}$ is estimated using the Cox & Munk model with wind and angles (Cox and Munk, 1954). $T_{\rm r+a}$ is calculated using look-up tables with certain aerosol model, aerosol optical thickness $\tau_{\rm a}$ and angles (Sun, 2005). To determine ρ_{mix}, mainly the aerosol contribution because $\rho_{\rm r}$ can be calculated in advance, $\tau_{\rm a}\longleftrightarrow\gamma$ ($\gamma = \rho_{\rm mix}/\rho_{\rm r}$) lookup tables with various aerosol models and angles are used (Sun and Guo, 2006; Antoine and Morel, 1999). Ten candidate aerosol models which are mainly based on four basic component mixing are adopted. The aerosol scattering phase function $P_{\rm a}(\Theta)$ and normalized aerosol optical thickness $\Delta\tau_{\rm a}$ are separately shown in Figs 1 and 2.

The water-leaving reflectance at two SWIR bands (centered at 1240 and 2130 nm) are assumed zeros. Thus, $\gamma(1240)$ and $\gamma(2130)$ are obtained from ρ_t. $\tau_{\rm a}(2130)_i$ for 10 aerosol models are calculated using $\tau_{\rm a}\longleftrightarrow\gamma$ lookup tables, and $\tau_{\rm a}(\lambda)_{\rm i}$ are extrapolated with the normalized optical thickness $\Delta\tau_a(\lambda)_{\rm i}$, and $\gamma(1240)_i$ are reversely calculated using $\tau_{\rm a}\longleftrightarrow\gamma$ lookup tables. Then, two aerosol models (represented with $i1$ and $i2$) most similar to the actual one are selected according to $\gamma(1240)_{\rm i1} < \gamma(1240) < \gamma(1240)_{\rm i2}$, and the mixing ratio X for interpolation between two aerosols is calculated as $[\gamma(1240) - \gamma(1240)_{\rm i1}]/[\gamma(1240)_{\rm i2} - \gamma(1240)_{\rm i1}]$. And then, for the visible and NIR bands, $\gamma(\lambda)_{\rm i1}$ and $\gamma(\lambda)_{\rm i2}$ are calculated from $\tau_{\rm a}(\lambda)_{\rm i1}$ and $\tau_{\rm a}(\lambda)_{\rm i2}$, and $\gamma(\lambda)$ is estimated as $(1 - X)\gamma(\lambda)_{\rm i1} + X\gamma(\lambda)_{\rm i2}$, and $\rho_{\rm mix}(\lambda)$ can then be calculated. Till now, $\rho_{\rm w}$ can be calculated from equation (1).

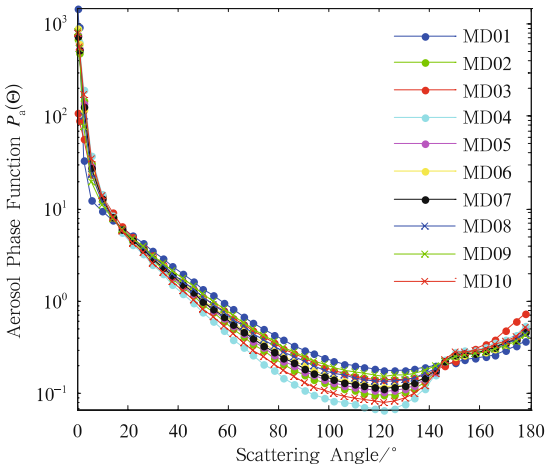

Fig.1. Aerosol scattering phase function for 551 nm band.

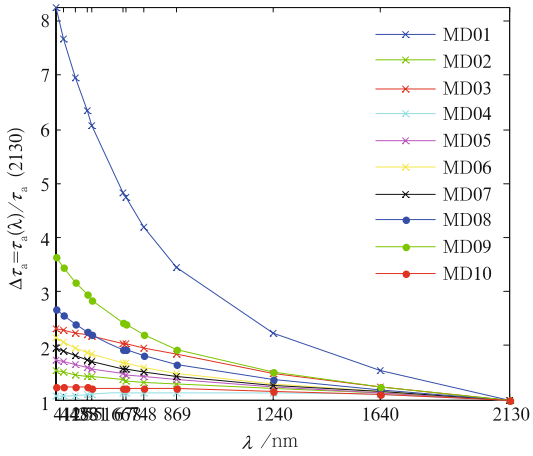

Fig.2. Normalized aerosol optical thickness.

2.2 *Chlorophyll-a concentration estimation model*

In situ chlorophyll-a concentrations were measured using HPLC method, and remote sensing reflectance spectra $R_{rs}(\lambda)$ from 350 to 1050 nm were derived from ASD measurements using above water method during the 2003 spring and fall cruises in the Yellow Sea and the East China Sea organized by the National Satellite Application Service (Tang et al., 2004). Using the 76 data collected in fall (the maximum, minimum and mean Chl-a values are 35.9, 0.2 and 2.2 mg/m^3, respectively), an empirical model is constructed as follows:

$$\mathrm{Log}_{10}(\mathrm{Chl}-a)=0.118445-3.05761\mathrm{Log}_{10}(X_c)+3.098626\mathrm{Log}_{10}^2(X_c)\quad(R^2=0.73),\quad(3)$$

$$X_c=[R_{rs}(443)/R_{rs}(551)][R_{rs}(412)/R_{rs}(488)]^{-0.8},\quad(4)$$

where R_{rs} is the MODIS band equivalent water remote sensing reflectance, which is calculated with the ASD measured $R_{rs}(\lambda)$ and MODIS Aqua spectral response function.

The model has been tested with in situ R_{rs} data. The root mean square percentage difference $\left(\sqrt{1/N\sum_{i=1}^{N}((X_i^{\mathrm{Mod}}-X_i^{\mathrm{Mea}})/X_i^{\mathrm{Mea}})^2}\right)$ is 45.3% for the 76 data used in model construction. When 83 data in spring (the maximum, minimum and mean Chl-a values are 15.2, 0.4 and 2.6 mg/m^3, respectively) are used for model testing, the root mean square percentage difference is 64.9%. Figure 3 provides the comparison between in situ Chl-a concentrations and model estimated Chl-a values from in situ R_{rs}. The results of linear fits for the data in fall and spring are also shown in the plot. The linear relationships between model estimated and in situ Chl-a are not very obvious with low correlation coefficient R^2.

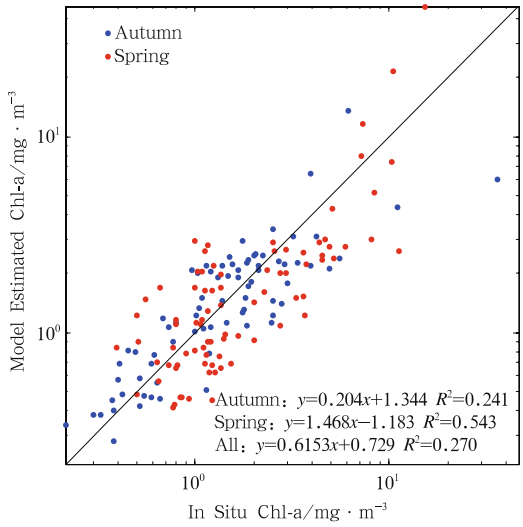

Fig.3. Model derived Chl-a values compared with in situ Chl-a concentrations.

3 Ocean color products around China coast

3.1 *MODIS ocean color products*

MODIS Aqua data have been processed for the China coastal region using the SWIR atmospheric correction and Chl-a algorithm described in section 2. For the data processing, the MOD35 products have been used for cloud masking. Ancillary data including wind, ozone and water vapour are from climatology dataset. The derived products include water-leaving reflectance, chlorophyll-a concentration, and aerosol optical thickness (AOT), etc.

The MODIS Aqua true color image around the China coast on October 19, 2003 (Fig. 4a) shows the very turbid waters along the China coast (brownish yellow to green in color), particularly the Hangzhou Bay, the Yangtze River Estuary, and the shoal along Jiangsu Province with extremely high sediment concentrations. Examples of the derived ocean color products corresponding to the MODIS data shown in Fig. 4a are also provided (Fig. 4b-h), which are the images of water-leaving reflectance $\rho_w(\lambda)$ at wavelengths 443, 488, 551, 667 and 869 nm, chlorophyll-a concentration (Chl-a), and aerosol optical thickness at 869 nm band $\tau_a(869)$, respectively. Values of $\rho_w(\lambda)$ from 443 to 667 nm bands (Fig. 4b-e) are scaled linearly from 0.0 to 0.15, while $\rho_w(869)$ (Fig. 4f) is scaled linearly from 0.0 to 0.05. Value of Chl-a (Fig. 4g) is scaled logarithmically from 0.09 to 30 (mg/m^3). Value of $\tau_a(869)$ (Fig. 4h) is scaled from 0.0 to 0.6.

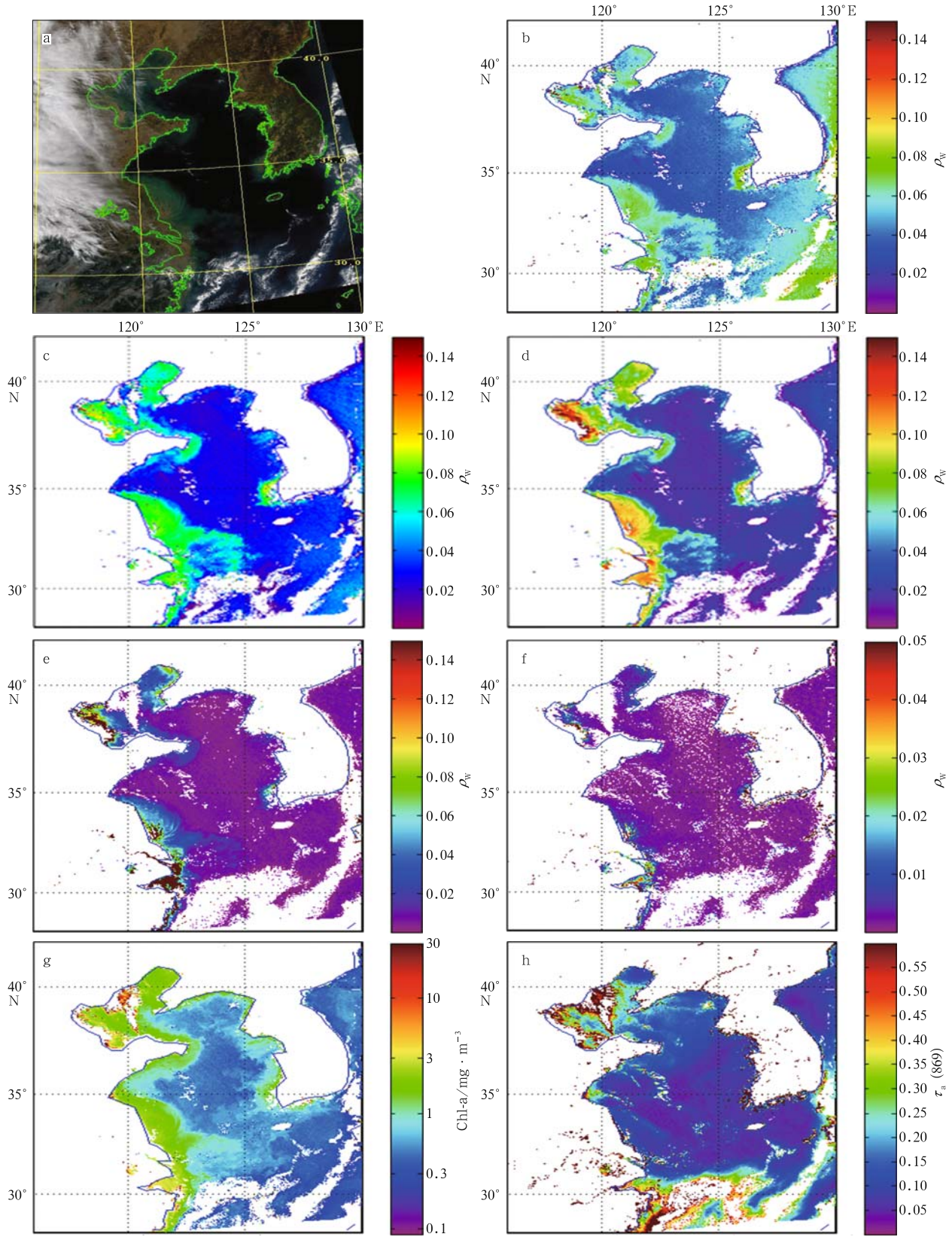

Fig.4. MODIS Aqua products on October 19, 2003 around the China coast for (a) true color image, (b-f) $\rho_w(\lambda)$ at 443, 488, 551, 667 and 869 nm bands, respectively, (g) Chl-a, and (h) $\tau_a(869)$.

It can be seen that, along the China coastal region, the MODIS derived $\rho_w(\lambda)$ value increases from blue to green. The extremely high value in 667nm (Fig. 4e) with brownish red color is due to the sensor saturation in this band. The NIR ocean contributions are significant, especially at the Hangzhou Bay, and some region in the Yangtze River Estuary and the shoal along Jiangsu Province.The MODIS-derived Chl-a values are in the reasonable range. And the results in Fig. 4 show no obvious correlations between the derived oceanic properties ($\rho_w(\lambda)$ and Chl-a) and atmospheric property, e.g., $\tau_a(869)$.

3.2 *MODIS products compared with in situ data*

The remote sensing reflectance spectra $R_{rs}(\lambda)$ derived from in situ measurements during 2003 spring and fall cruises in the Yellow Sea and the East China Sea are taken to be compared with those from MODIS-derived $\rho_w(\lambda)$ after the conversion of $R_{rs}(\lambda)$=$\rho_w(\lambda)/\pi$. Figure 5 shows the scatter diagram between in situ and MODIS derived $R_{rs}(\lambda)$ values at the nine MODIS bands. The MODIS data are the average of pixels within ±0.015° centred at the in situ data location. In situ data acquired within ±6 hours centred at the MODIS measurement time are included with a total of 20 match-ups. Although there are some noises, the results in Fig. 5 show a relatively good linear relationship between MODIS and in situ $R_{rs}(\lambda)$. The slope of the linear fit for all the nine bands is 1.093, the intercept is 0.000702 and the correlation coefficient R^2 is 0.923. The results of linear fits for 412, 443, 488, 531, 551, 667, 678, 748 and 869 nm bands are also shown in the plot, indicating more noise at the 412, 443 and 748 nm band. The MODIS derived $R_{rs}(\lambda)$ tends to be overestimated at 412 and 443 nm bands which may be subject to the radiative transfer precision and improper aerosol models. The root mean square errors (RMSE) of $R_{rs}(\lambda)$ are 0.0054, 0.0054, 0.0032, 0.0029, 0.0036, 0.00095, 0.00094, 0.0010 and 0.0004 sr^{-1} for 412, 443, 488, 531, 551, 667, 678, 748 and 869 nm bands, respectively. The RMSE for all dataset is 0.0031 sr^{-1}.

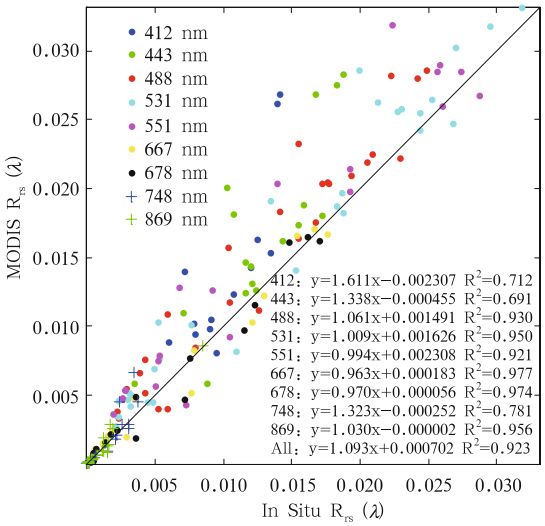

Fig.5. MODIS derived remote sensing reflectance values compared with in situ data for the bands of 412, 443, 488, 531, 551, 667, 678, 748 and 869 nm.

Four sites among the 20 match-ups are selected to give the $R_{rs}(\lambda)$ spectral comparison examples in Fig.6.The turbidity of these four sites is medium to high with the total suspended matter (TSM) concentration of 14.2, 13.2, 10.4 and 117.9 mg/L. The in situ hyper-spectral $R_{rs}(\lambda)$, MODIS band equivalent values from in situ measurement, MODIS-derived R_{rs} from NASA standard product (from http://oceancolor.gsfc.nasa.gov), and MODIS-derived R_{rs} from the SWIR atmospheric correction algorithm are shown. The location in latitude and longitude, and time difference between MODIS and in situ measurements are also indicated in each plot. It shows in Fig. 6 that the SWIR atmospheric correction performs reasonably well for these turbid waters. The in situ data shows high remote sensing reflectance values in NIR bands (748 and 869 nm), i.e., the NIR $R_{rs}(\lambda)$ values range from 0.003 to 0.016. The derived R_{rs} from NASA standard product tends to be underestimated in waters with medium turbidity. At site HD41, no valid retrievals are available from the NASA standard product because of the high TSM loading, while reasonable values could be derived using the SWIR algorithm (no values in 551,667, 678 and 748 nm bands because of band saturation).

The HPLC measured in situ chlorophyll-a concentration collected during the 2003 spring and fall cruise in the Yellow Sea and the East China Sea are taken to be compared with the MODIS-derived Chl-a. The root mean square percentage differences $\left(\sqrt{1/N\sum_{i=1}^{N}((X_i^{\mathrm{Mod}}-X_i^{\mathrm{Mea}})/X_i^{\mathrm{Mea}})^2}\right)$ are 45.5% and 47.1% for data in fall and spring, respectively. The root mean square percentage difference for all dataset is 46.1%. Fig. 7 provides the comparison between the in situ and MODIS derived Chl-a values. The results of linear fits for the data in fall and spring are also

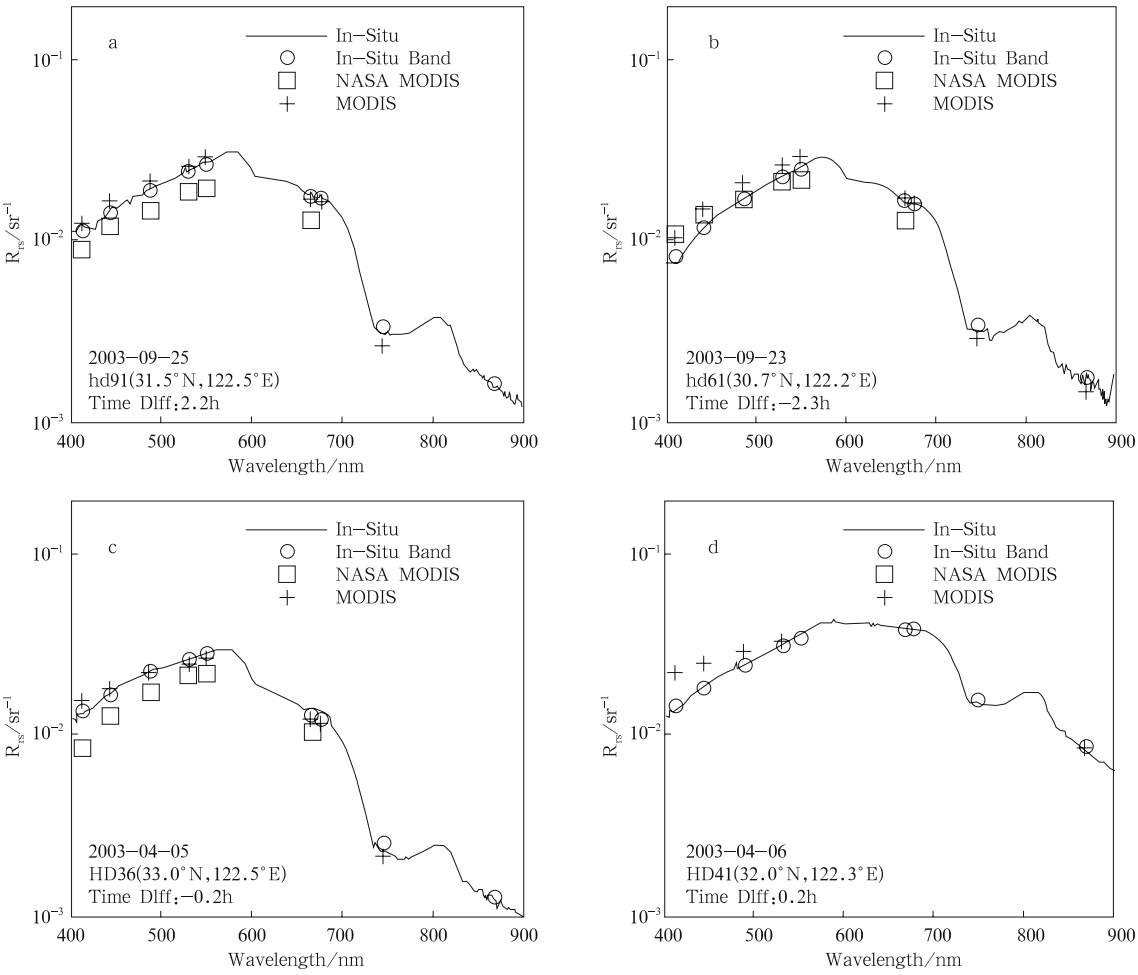

Fig.6. MODIS derived remote sensing reflectance spectra compared with those from in situ data acquired on (a) September 25, 2003, (b) September 23, 2003, (c) April 5, 2003, and (d) April 6, 2003.

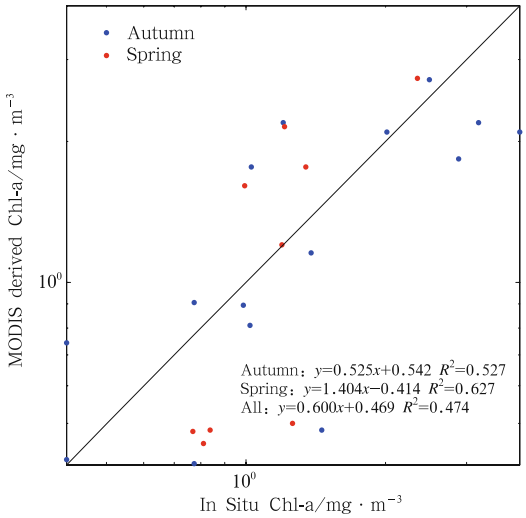

Fig.7. MODIS derived Chl-a values compared with in situ Chl-a concentrations.

shown in the plot. Similar with the result of model estimation from in situ R_{rs} shown in Fig. 3, there is not a good linear relationship between MODIS derived and in situ Chl-a. Sun et al. (2009) has found that the Chl-a values from NASA standard product are systematically overestimated. The root mean square percentage difference is 145.46%. The major reason for this poor performance is the OC3 model (coefficients) unsuitability. In comparison, the performance of the algorithms in this paper is much better.

4 Conclusions

We have presented the SWIR atmospheric correction and Chl-a concentration estimation model for MODIS ocean color processing and used them to derive the MODIS Aqua water-leaving reflectance spectra and Chl-a along the China coastal region. In these turbid and optically complex waters, the standard MODIS ocean color products tend to have invalid values. By image analysis and comparing our

MODIS derived ocean color products with those from in situ measurements collected in the Yellow Sea and the East China Sea, reasonably good results have been obtained. It is obvious that along the China coast with high sediment loadings, water-leaving reflectance in the NIR bands is significant. The satellite derived and in-situ reflectance spectra can match in the turbid waters along China coast, and there are relatively good linear relationship between satellite derived and in-situ reflectance in most of ocean color bands. The RMSE values of $R_{\mathrm{rs}}(\lambda)$ are 0.0054, 0.0054, 0.0032, 0.0029, 0.0036, 0.00095, 0.00094, 0.0010 and 0.0004 sr^{-1} for 412, 443, 488, 531, 551, 667, 678, 748 and 869 nm bands, respectively, and 0.0031 for all dataset. The satellite-derived Chl-a values are in the reasonable range and the root mean square percentage difference is 46.1%.

References

Antoine D, Morel A. 1999. A multiple scattering algorithm for atmospheric correction of remotely sensed ocean color (MERIS instrument): principle and implementation for atmospheres carrying various aerosols including absorbing ones. Int J Remote Sens, 20(9): 1875–1916

Cox C, Munk W. 1954. Measurements of the roughness of the sea surface from photographs of the Sun's glitter. J Opt Soc Am, 44(11): 838–850

Gordon H R, Wang M. 1994. Retrieval of water-leaving radiance and aerosol optical thickness over the oceans with SeaWiFS: a preliminary algorithm. Appl Opt, 33(3): 443–452

Gordon H R. 1997. Atmospheric correction of ocean color imagery in the earth observing system era. J Geophys Res, 102(D14): 17081–17106

Koepke P. 1984. Effective reflectance of oceanic whitecaps. Appl Opt, 23(11): 1816–1824

Lavender S J, Pinkerton M H, Moore G F, et al. 2005. Modification to the atmospheric correction of SeaWiFS ocean color imagers over turbid waters. Continental Shelf Research, 25: 539–555

O'Reilly J E, Maritorena S, Mitchell B G. 1998. Ocean color chlorophyll algorithms for SeaWiFS. J Geophys Res, 103(C11): 24937–24953

Ruddick K G, Ovidio F, Rijkeboer M. 2000. Atmospheric correction of SeaWiFS imagery for turbid coastal and inland waters. Appl Opt, 39(6): 897–912

Siegel D A, Wang M, Maritorena S. 2000. Atmospheric correction of satellite ocean color imagery: The black pixel assumption. Appl Opt, 39(21): 3582–3591

Stumpf R P, Arnone R A, Gould R W, et al. 2003. A partially coupled ocean-atmosphere model for retrieval of water-leaving radiance from SeaWiFS in coastal waters. In S B Hooker & E R Firestone(Eds.), NASA Tech. Memo. 2003-206892 SeaWiFS Postlaunch Technical Report Series, v 22: 51-59. Greenbelt, Maryland: NASA Goddard Space Flight Center

Sun L, Guo M. 2006. Atmospheric correction for HY-1A CCD in Case 1 waters. In: Proceedings of SPIE, Remote Sensing of the Environment: 15th National Symposium on Remote Sensing of China, Guiyang, China, v: 6200: 20–31

Sun L, Zhang J, Guo M. 2006. Rayleigh lookup tables for HY-1A CCD data processing. J Remote Sens (in Chinese), 10(3): 306–311

Sun L, Zhang J. 2007. Analysis of influence of gaseous absorption on "HY-1A" CCD data: simulation and correction for Rayleigh scattering. Acta Oceanologica Sinica (in Chinese), 29(3): 137–145

Sun L. 2005. Atmospheric correction and water constituent retrieval for HY-1A CCD. PhD dissertation (in Chinese). Qingdao: Institute of Oceanology, Chinese Academy of Science, 67–69

Sun Ling, Wang Xiaomei, Guo Maohua, et al. MODIS ocean color product validation around the Yellow Sea and East China Sea. J Lake Sci (In Chinese), 2009, v 21(2): 143-148 Tang J, Wang X, Song Q, et al. 2004. The statistic inversion algorithms of water constituents for the Huanghai Sea and the East China Sea. Acta Oceanologica Sinica, 23(4): 617–626

Wang M, Tang J, Shi W. 2007. MODIS-derived ocean color products along the China east coastal region. Geophysical Research Letters, v 34, L06611, doi:10.1029/2006GL028599 Wang M. 2007. Remote sensing of the ocean contributions from ultraviolet to near-infrared using the shortwave infrared bands: simulations. Applied Optics, 46(9): 1535–1547